Eur Radiol (2011) 21:1651–1657
DOI 10.1007/s00330-011-2108-4

MAGNETIC RESONANCE

4D-MR flow analysis in patients after repair for tetralogy of Fallot

J. Geiger · M. Markl · B. Jung · J. Grohmann · B. Stiller · M. Langer · R. Arnold

Received: 11 January 2011 / Revised: 27 January 2011 / Accepted: 4 February 2011 / Published online: 29 March 2011

Abstract

Objectives Comprehensive analysis of haemodynamics by 3D flow visualisation and retrospective flow quantification in patients after repair of tetralogy of Fallot (TOF).

Methods Time-resolved flow-sensitive 4D MRI (spatial resolution ~ 2.5 mm, temporal resolution = 38.4 ms) was acquired in ten patients after repair of TOF and in four healthy controls. Data analysis included the evaluation of haemodynamics in the aorta, the pulmonary trunk (TP) and left (lPA) and right (rPA) pulmonary arteries by 3D blood flow visualisation using particle traces, and quantitative measurements of flow velocity.

Results 3D visualisation of whole heart haemodynamics provided a comprehensive overview on flow pattern changes in TOF patients, mainly alterations in flow velocity, retrograde flow and pathological vortices. There was consistently higher blood flow in the rPA of the patients (rPA/lPA flow ratio: 2.6±2.5 vs. 1.1±0.1 in controls). Systolic peak velocity in the TP was higher in patients (1.9 m/s±0.7 m/s) than controls (0.9 m/s±0.1 m/s).

Conclusions 4D flow-sensitive MRI permits the comprehensive evaluation of blood flow characteristics in patients after repair of TOF. Altered flow patterns for different surgical techniques in the small patient cohort may indicate its value for patient monitoring and potentially identifying optimal surgical strategies.

Keywords 4D MRI · Tetralogy of Fallot · Pulmonary haemodynamics · Vortices · Monitoring

Electronic supplementary material The online version of this article (doi:10.1007/s00330-011-2108-4) contains supplementary material, which is available to authorized users.

J. Geiger (✉) · M. Markl · B. Jung · M. Langer
Department of Radiology, Medical Physics,
University Hospital Freiburg,
Hugstetter Str. 55,
79106 Freiburg, Germany
e-mail: julia.geiger@uniklinik-freiburg.de

J. Grohmann · B. Stiller · R. Arnold
Department of Congenital Heart Disease and Pediatric Cardiology,
University Hospital Freiburg,
Mathildenstr. 1,
79106 Freiburg, Germany

Introduction

Tetralogy of Fallot (TOF), the most common cyanotic congenital heart defect, accounts for about 10% of all congenital heart diseases [1, 2]. These patients usually undergo surgery in the first year of life with a good clinical outcome. The number of long-term survivors requiring cardiac and vascular imaging for follow-up and circulatory monitoring continues to rise [3]. Pulmonary valve insufficiency with consecutive right ventricular volume overload is the most common and serious postoperative problem in patients with TOF [4, 5]. Conventional angiography during cardiac catheterisation used to be considered the gold standard for the evaluation of pulmonary function, but Magnetic Resonance Imaging (MRI) has evolved as a powerful method for evaluating cardiovascular function after surgery for tetralogy of Fallot [6, 7]. Both angiography and standard MRI protocols, however, provide neither a complete picture nor detailed information about 3D haemodynamics and flow alterations occurring in the right ventricular outflow tract and the entire pulmonary vascular system at different points in time.

Time-resolved 3D phase-contrast MRI with three-directional velocity encoding, also known as flow-sensitive 4D-MRI, has become a valuable method for comprehensively assessing vascular haemodynamics in the aorta and other vascular territories [8–12]. In this study, the feasibility of whole heart flow-sensitive 4D-MRI [13, 14] for the visualisation of 3D flow characteristics and flexible retrospective flow quantification was evaluated in ten paediatric patients after repair of TOF. It was the aim to visualise and understand changes in blood flow characteristics in the pulmonary arteries after complex surgical repair.

Materials and methods

Patients

Ten patients after repair of TOF (age 12.1±8.1 years, range 2–24 years, 5 male) and four healthy controls (age 26±0.8 years, range 25–27 years) underwent whole heart flow-sensitive 4D-MRI. The mean interval between surgery and MRI was 10.4±7.9 years. The mean age of corrective surgery was 0.8±1.2 years. Four patients underwent trans-annular repair with consecutive pulmonary valve insufficiency, four pulmonary valve-preserving surgery, and two valve conduit implantation. The study was approved by our local ethics committee, and written informed consent was obtained from each participant and his or her parents prior to MRI examinations.

Magnetic resonance imaging

MRI examinations were performed on 1.5T (eight patients) and 3T MR (two patients and four controls) systems (AVANTO or TRIO, Siemens, Germany). Flow-sensitive 4D-MRI acquisitions were synchronised to the heart rate and breathing using prospective ECG-gating and adaptive diaphragm navigator gating [9]. The MRI sequence consisted of a k-space segmented rf-spoiled gradient echo sequence with interleaved 3-directional velocity encoding. Data were acquired in a sagittal oblique 3D data volume individually adapted to include the entire heart, thoracic aorta, and main pulmonary arteries. Imaging parameters were as follows: velocity sensitivity = 150–200 cm/s, TE = 2.3–2.5, TR = 4.7–5.1, field of view (FOV) = 125–345 mm×250–460 mm, spatial resolution = 1.7–2.2×1.8–3.2×1.6–2.5 mm³, temporal resolution = 37.6–40.8 ms, flip angle = 7°–15°, scan time ~10–20 min, parallel imaging with reduction factor R = 2 [15].

3D flow visualisation

Data analysis included calculation of a 3D phase contrast (PC) MR angiogram (MRA) from 4D-MRI data combined with 3D blood-flow visualisation using commercially available software (EnSight, CEI, Apex, NC, USA). Visualisation of aortic and pulmonary flow was achieved by traces of 3D virtual particles demonstrating time-resolved blood flow [16, 17]. Particle traces were emitted from interactively positioned planes in the ascending aorta (AAo), main pulmonary artery (TP), and right (rPA) and left pulmonary arteries (lPA). Traces along the measured velocities were colour-coded according to the local velocity in the different vessels of interest.

Flow pattern analysis

4D-blood flow visualisation was evaluated for each patient in consensus reading with regard to vortex formation, retrograde flow, and the presence of increased peak velocities. Time-resolved 3D particle traces were viewed dynamically and rotated or magnified for inspection in any chosen orientation as illustrated in the supplemental video. As illustrated in Fig. 1, vortices were defined as regional circular flow patterns deviating by more than 90° from the physiological flow direction along the vessel lumen. Vortex severity was graded in 3 categories: no vortex formation = 0, moderate vortex (flow rotation <360°) = 1, pronounced vortex (flow rotation >360°) = 2. Retrograde flow in the right ventricular outflow tract, right and left pulmonary arteries as well as the ascending aorta was evaluated using a 3-grade ranking: no retrograde flow = 0, moderate retrograde flow = 1, severe retrograde flow = 2. Presence of high peak velocities, defined as flow velocity >1.5 m/s, was evaluated as absent = 0 or evident = 1.

Flow quantification

Blood flow was quantified by retrospectively extracting the measured flow velocities in manually-positioned analysis planes from the flow-sensitive 4D-MR data [18]. Flow-time curves, total flow, and systolic peak velocities were analysed in the AAo approximately 1 cm above the aortic valve, in the TP above the pulmonary valve, and in the middle segment of the rPA and lPA. Flow-time curves were used to calculate the retrograde flow fraction in all vessels. Total flow to the left and right pulmonary arteries was used to derive the rPA/lPA flow ratio.

Results

3D blood flow visualisation

We observed a marked variation in flow characteristics in all patients, as exemplified in Fig. 1 (severe vortex formation) and 2 (severe retrograde flow and rPA/lPA flow asymmetry). See supplemental video (Fig. 5) depicting vortices of Fig. 1.

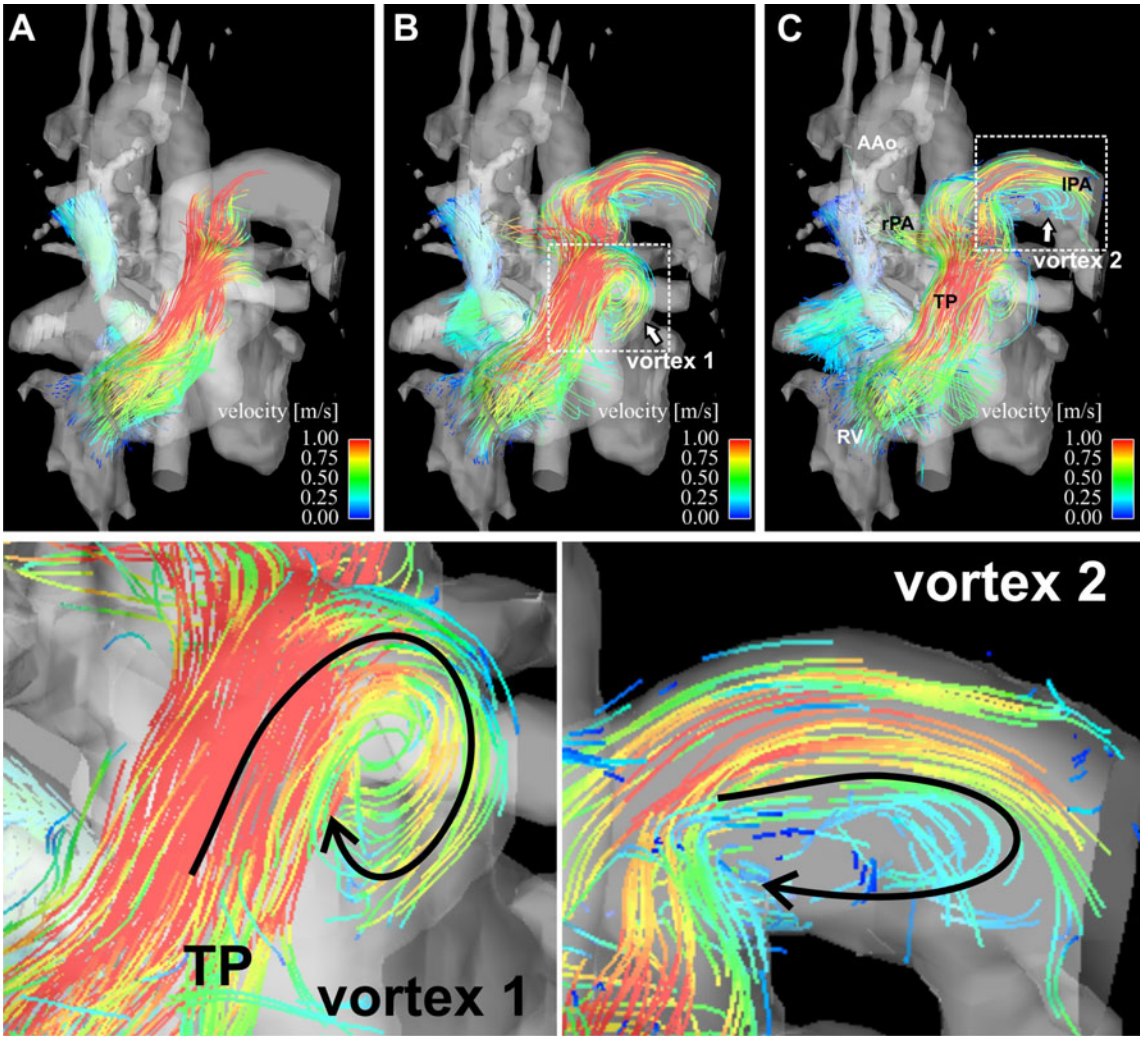

Fig. 1 Top row: 3D particle trace visualisation illustrating the dynamics of right ventricular outflow for three successive systolic time-frames (A-C). High systolic velocities (*red colour*) and vortex flow in the pulmonary trunk (TP) and the left pulmonary artery (lPA) can clearly be appreciated (*white arrows*). Lower row: Magnification of vortex flow in the TP (vortex 1) and lPA (vortex 2). Pronounced vortex formation (vortex 1, grading = 2) in the TP coincided with a bulging enlargement of the outflow tract encompassing the circular flow. Additional vortex flow (vortex 2, grading = 2 was observed immediately distal to the lPA's branching point. 3D blood flow dynamics can be best appreciated in the supplemental video (Fig. 5). AAo: ascending aorta, RV: right ventricle, rPA: right pulmonary artery

Mean vortex severity in the TP was 0.9±1.0 in patients, with less severe vortices in the rPA (0.2±0.7) and lPA (0.7±0.9). Pronounced vortices (grade 2) in the TP were detected in four patients and moderate vortices (grade 1) in two patients. Three patients presented mild-to-moderate vortices in the aorta. Flow visualisation in the aorta was impaired in one patient because of poor overall image quality. Evaluation of the pulmonary arteries was hindered in two patients due to artefacts caused by a stent within the lPA.

High peak velocities >1.5 m/s in the TP were apparent in eight patients (average grading = 0.8±0.4) and in the rPA and lPA in seven and six patients, respectively (Fig. 2). One patient had high flow velocities in the ascending aorta.

All patients presented unmistakable retrograde flow in the TP due to pulmonary insufficiency (average grading = 1.8±0.4) estimated as moderate (grade 1) in two and severe (grade 2) in eight TOF patients (Fig. 2). Eight patients had retrograde flow in the rPA (average grading = 1.8±0.7, two moderate, six severe) and the lPA (average grading = 1.4±0.7, three moderate, five severe). No regurgitation was detected in the aorta.

Flow velocities above 1.5 m/s, vortices, and retrograde flow were not detected in the healthy volunteer group.

Flow quantification

Flow-time curves averaged over patients and controls in the aorta and pulmonary arteries are displayed in Fig. 3. As

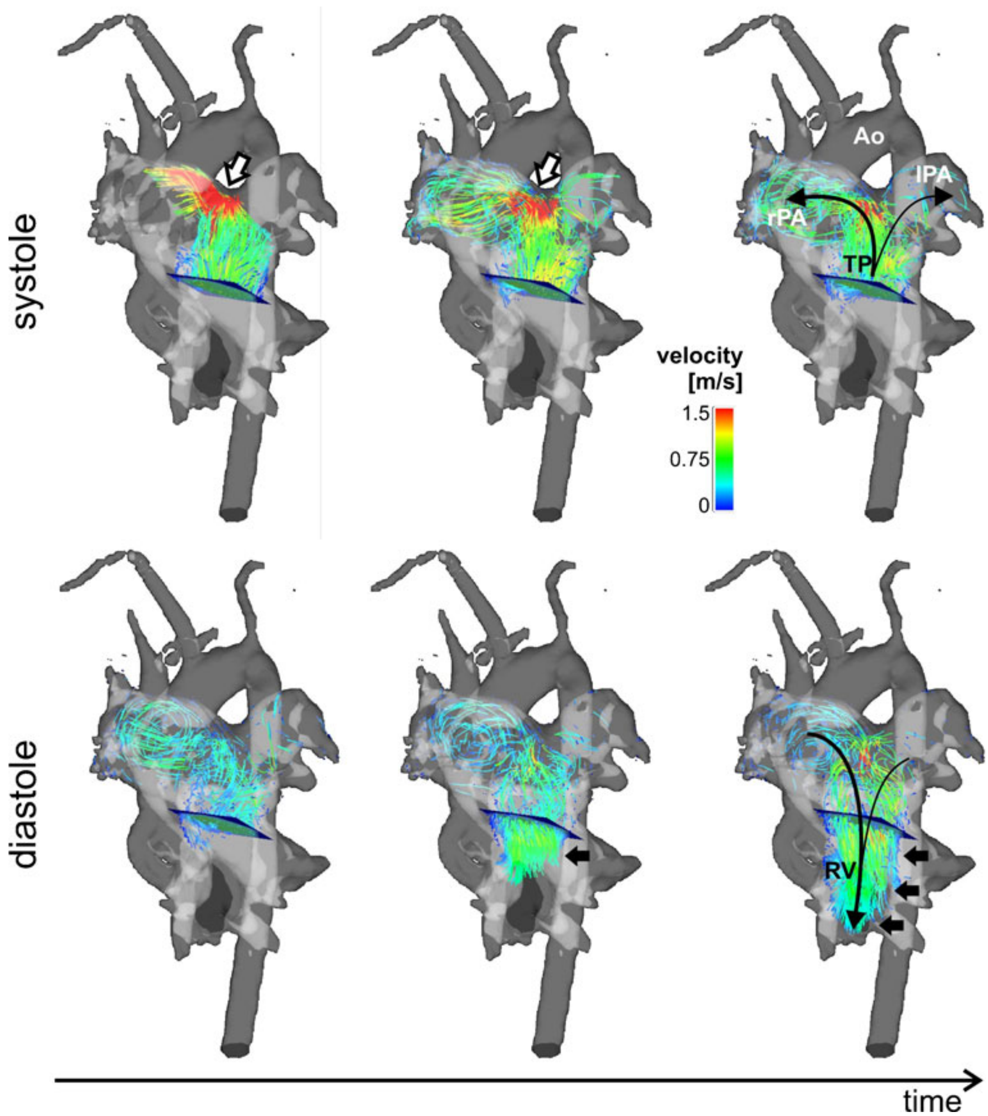

Fig. 2 Time evolution of blood flow in the right ventricular outflow tract and pulmonary arteries during one cardiac cycle visualised by 3D particle traces originating from an emitter plane at the level of the pulmonary valve. Substantial flow acceleration during systole is clearly evident (*white arrows* and *red colours* = velocities >1.5 m/s). Pulmonary valve insufficiency resulted in marked diastolic retrograde flow (*small black arrows*, retrograde fraction = 39% in this patient example) into the right ventricle (RV). During both systole and diastole, particle traces visualised marked asymmetry of flow to and from the left (lPA) compared to the right (rPA) pulmonary artery. This finding was confirmed by quantitative analysis which revealed the highest rPA/lPA flow ratio = 8.2 in the study cohort, TP: pulmonary trunk, Ao: aorta

expected, we noted strong regurgitation in the TOF patients' pulmonary arteries (regurgitation fraction = 29%±11%) whereas no regurgitation was observed in controls. Systolic peak velocity in the pulmonary trunk was higher in patients (1.9 m/s±0.7 m/s) than controls (0.9 m/s±0.1 m/s), while aortic peak velocities were similar (1.4 m/s±0.3 m/s in patients versus 1.3 m/s±0.1 m/s in controls). The rPA/lPA flow ratio was noticeably variable in TOF patients, with a tendency to higher blood flow in the rPA (rPA/lPA flow ratio = 2.6±2.5). In contrast, the control group's blood flow was similar in both pulmonary arteries (rPA/lPA flow ratio = 1.1±0.1).

To test the internal consistency of flow quantification based on flow-sensitive 4D MRI data, net aortic flow was compared to net pulmonary trunk flow and net pulmonary trunk flow was compared to net (RPA+LPA) flow using correlation analysis. As summarized in Table 1, significant ($p<0.01$) and high correlation ($r>0.9$) confirms the validity of the MR flow analysis.

Comparison of haemodynamics according to surgical repair technique

As illustrated in Fig. 4, groups were divided into healthy controls and patients with transannular (1), valve-preserving (2) and conduit repair (3). There was an obvious tendency towards higher regurgitation fractions in the lPA and rPA after transannular repair. No noticeable trends were found for vortex formation, rPA/lPA flow ratio, or peak velocities.

Discussion

The feasibility of whole heart 4D-MRI for the comprehensive evaluation of pulmonary haemodynamics was successfully demonstrated in a small cohort of children, teenagers and young adults who had undergone TOF repair. In contrast to older normal controls, potentially pathologic

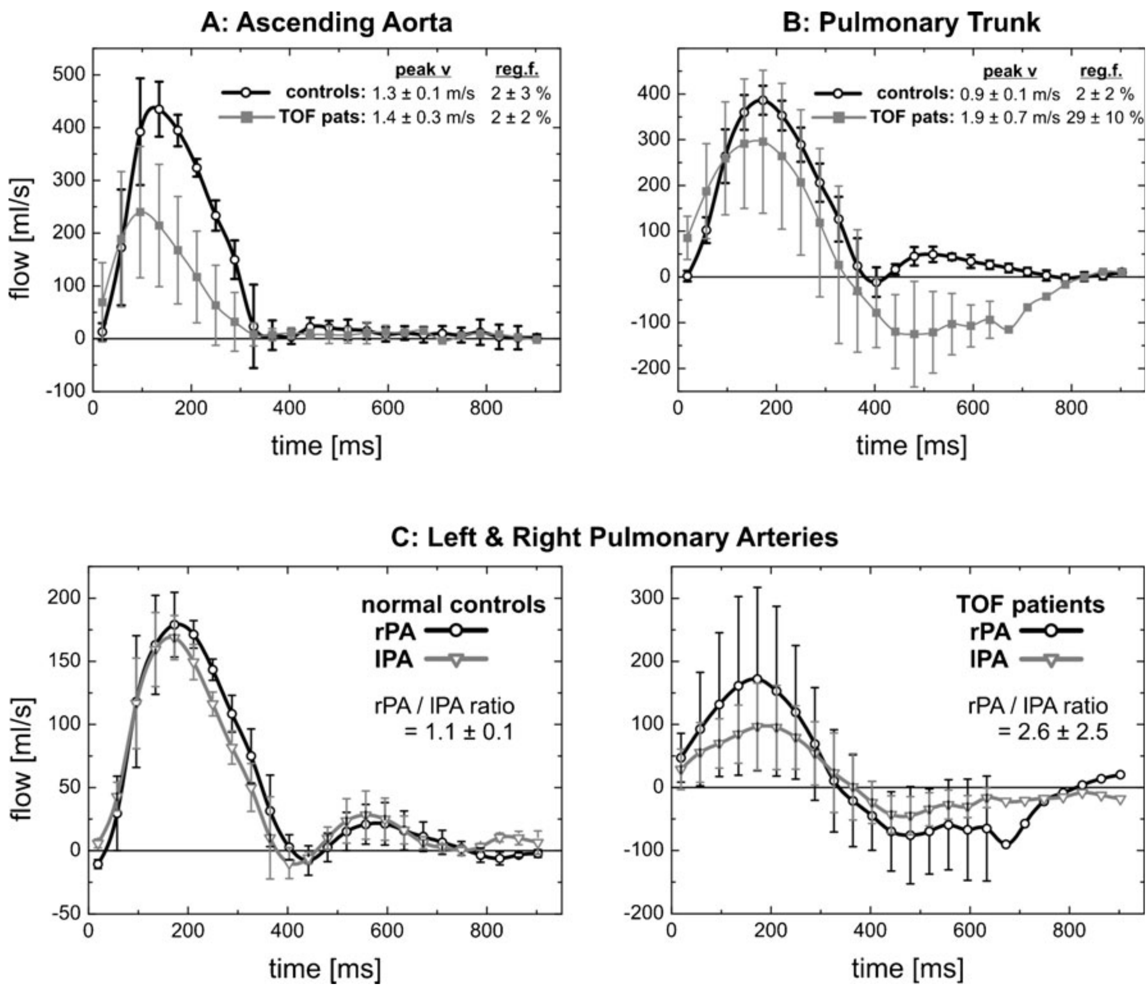

Fig. 3 Averaged blood flow-time curves in 10 patients with tetralogy of Fallot (TOF) and 4 normal subjects. **a**: Pulsatile flow-time curves in the ascending aorta (AAo) **b**: Flow-time curves in the pulmonary trunk clearly show regurgitant flow due to valve insufficiency in the TOF patient **c**: Flow to the left and right pulmonary arteries differed considerably between normal controls and TOF patients. In comparison to volunteers, TOF patients showed pronounced diastolic retrograde flow and enhanced and more variable flow ratio to the left and right lung

vortex flow, substantial flow acceleration, pulmonary regurgitation, and abnormal flow ratios between right and left pulmonary arteries were our main findings.

In TOF patients, residual pulmonary stenosis, especially branch stenosis, and pulmonary regurgitation are the main problems in mid- and long-term follow-up. Progressive right ventricular dilatation or reduced ventricular function is an indicator of the need for valve replacement [19]. MRI is well suited to assess pulmonary vessel anatomy, using predominantly transverse black blood sequences such as HASTE or bright blood sequences, e.g. SSFP, or MRA, as recommended in the literature [6, 7, 20, 21]. Data available from echocardiography, however, are often incomplete, because pulmonary arteries are generally difficult to evaluate due to acoustic-window limitations [22]. We used the advantages of 4D-MRI, including complete volumetric coverage of the pulmonary trunk and flow-sensitive information on 3D blood flow to evaluate pulmonary haemodynamics, overcome the regionally-limited results of 2D phase-contrast MRI, and improve understanding of postoperative flow alterations [23].

Table 1 Comparison of net flows in the ascending aorta (AAo), pulmonary trunk (TP) and left and right pulmonary arteries (LPA und RPA)

Net flow [ml/cycle]		correlation	
AAo	TP	p-value	r-value
55.6±28.0	59.9±29.0	< 0.01	0.95
TP	RPA+LPA		
59.9±29.0	57.8±22.8	< 0.01	0.91

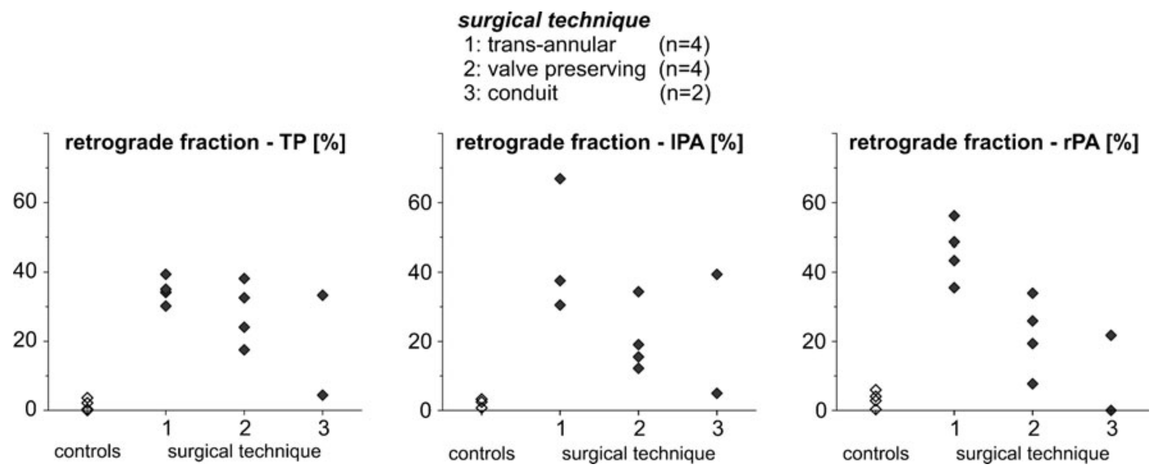

Fig. 4 Comparison of haemodynamic parameters between healthy volunteers (controls) and patients grouped according to the surgical technique employed for repair of tetralogy of Fallot (TOF)

The information on flow differences to the left and right lung found in our small patient cohort is similar to findings in previous studies [24, 25]. Using Doppler echocardiography data as a reference, normal pulmonary peak velocities range between 0.3 and 1.0 m/s, depending on the author [26–28]. In our survey, elevated peak velocities averaged 1.86 m/s in the patient group. No residual pulmonary stenosis, which could be the cause for flow acceleration, was detected in our investigation. We therefore assume that increased flow velocities may be compensating for blood reflux caused by pulmonary insufficiency which is a frequent long-term anomaly in 73% of TOF patients after repair [29].

A remarkable finding was the appearance of vortex flow patterns which cannot be detected by standard MRI scans or echocardiography. Reiter et al. detected a correlation between pulmonary hypertension and the appearance of vortex flow, followed by elevated pulmonary arterial pressure [30]. On the other hand, preexisting vortices may lead to pulmonary artery dilation. This concept is confirmed by previous 4D-MRI studies of the aorta, showing that vortices are associated with shear force alterations on the vessel wall, thus leading to changes in endothelial function, which is a predisposing factor for vascular remodelling and aortic dilatation [31, 32]. Similarly, pulmonary trunk abnormalities may influence the development of regurgitation and haemodynamic alterations. Using 4D-MR flow analysis, the complexity of vascular haemodynamics and its influence on morphology and function may be investigated more precisely than is possible using any other imaging tool.

Finally, we investigated the impact of the type of surgical repair and 4D-MR flow patterns. Although the number of patients in each group was limited, we found that transannular repair influences haemodynamics with regard to regurgitation. Hence, when considering the long-term sequelae suffered by TOF patients, and current discussions concerning the ideal time for valve replacement [33, 34], patients' outcome might be additionally affected by the postoperative vessel dilation caused by vortices.

This study is limited by the small number of patients and the absence of an age matched control group. Larger patient cohorts and further follow-up examinations of our patients and long-term studies will be essential to learn more about the pathophysiological impact of the altered pulmonary haemodynamics and their link to prognostic and therapeutic consequences. Note that a validation of flow quantification based on the 4D data against standard flow measurements using the conventional 2D phase contrast MRI was not performed in the presented subjects. In a previous study we have demonstrated close agreement for flow derived from standard time-resolved 2D and 4D data [18]. A further disadvantage of the presented MRI methods is related to the long overall scan times on the order of 10–20 min which can be addressed using advanced parallel imaging techniques [35]. Nevertheless, we believe that the possibility for comprehensive visualisation of 3D haemodynamics and flexible retrospective flow quantification at any site within the 3D imaging volume justifies long scan times in cases of complex cardiac and vascular alterations as for TOF.

Conclusions

Beyond its unique potential to demonstrate the complexity of vascular morphology and function in TOF patients, 4D-MR flow analysis may prove valuable in clinical routine in the future by providing important data on both intracardiac and pulmonary vascular flow.

Acknowledgement Dr. Markl receives funding from the "Deutsche Forschungsgemeinschaft" (DFG) Grant # MA 2383/5-1 and Bundesministerium für Bildung und Forschung (BMBF), Grant # 01EV0706.

References

1. Gatzoulis MA (2003) Tetralogy of Fallot. In: Gatzoulis M, Webb G, Daubeney P (eds) Diagnosis and management of adult congenital heart disease. Elsevier, London, pp 315–326
2. Therrien J, Webb G (2003) Clinical update on adults with congenital heart disease. Lancet 362:1305–1313
3. Apitz C, Webb GD, Redington AN (2009) Tetralogy of Fallot. Lancet 274:1462–1471
4. Huehnergarth KV, Gurvitz M, Stout KK et al (2008) Repaired tetralogy of Fallot in the adult: monitoring and management. Heart 94:1663–1669
5. Davlouros PA, Kilner PJ, Hornung TS et al (2002) Right ventricular function in adults with repaired tetralogy of Fallot assessed with cardiovascular magnetic resonance imaging: detrimental role of right ventricular outflow aneurysms or akinesia and adverse right-to-left ventricular interaction. J Am Coll Cardiol 40:2044–2052
6. Kilner PJ, Geva T, Kaemmerer H et al (2010) Recommendations for cardiovascular magnetic resonances in adults with congenital heart disease from the respective working groups of the European Society of Cardiology. Eur Heart J 31:794–805
7. Norton KI, Tong C, Glass RB et al (2006) Cardiac MR imaging assessment following tetralogy of Fallot repair. Radiographics 26:197–211
8. Wigstrom L, Sjoqvist L, Wranne B (1996) Temporally resolved 3D phase-contrast imaging. Magn Reson Med 36:800–803
9. Markl M, Harloff A, Bley TA et al (2007) Time-resolved 3D MR velocity mapping at 3T: improved navigator-gated assessment of vascular anatomy and blood flow. J Magn Reson Imaging 25:824–831
10. Hope MD, Meadows AK, Hope TA et al (2010) Clinical evaluation of aortic coarctation with 4D flow MR imaging. J Magn Reson Imaging 31:711–718
11. Harloff A, Albrecht F, Spreer J et al (2009) 3D blood flow characteristics in the carotid artery bifurcation assessed by flow-sensitive 4D MRI at 3T. Magn Reson Med 61:65–74
12. Boussel L, Rayz V, Martin A et al (2009) Phase-contrast magnetic resonance imaging measurements in intracranial aneurysms in vivo of flow patterns, velocity fields, and wall shear stress: comparison with computational fluid dynamics. Magn Reson Med 61:409–417
13. Uribe S, Beerbaum P, Sorensen TS et al (2009) Four-dimensional (4D) flow of the whole heart and great vessels using real-time respiratory self-gating. Magn Reson Med 62:984–992
14. Markl M, Geiger J, Kilner P et al (2010) Time-resolved three-dimensional magnetic resonance velocity mapping of cardiovascular flow paths in volunteers and patients with Fontan circulation. Eur J Cardiothorac Surg 39:206–212
15. Griswold MA, Jakob PM, Heidemann RM et al (2002) Generalized autocalibrating partially parallel acquisitions (GRAPPA). Magn Reson Med 47:1202–1210
16. Buonocore MH (1998) Visualizing blood flow patterns using streamlines, arrows, and particle paths. Magn Reson Med 40:210–226
17. Frydrychowicz A, Harloff A, Jung B et al (2007) Time-resolved, 3-dimensional magnetic resonance flow analysis at 3T: visualization of normal and pathological aortic vascular hemodynamics. J Comput Assist Tomogr 31:9–15
18. Stalder AF, Russe MF, Frydrychowicz A et al (2008) Quantitative 2D and 3D phase contrast MRI: optimized analysis of blood flow and vessel wall parameters. Magn Reson Med 60:1218–1231
19. Adamson L, Vohra HA, Haw MP (2009) Does pulmonary valve replacement post repair of tetralogy of Fallot improve right ventricular function? Interact Cardiovasc Thorac Surg 9:520–527
20. Lorenz CH (2000) The range of normal values of cardiovascular structures in infants, children, and adolescents measured by magnetic resonance imaging. Pediatr Cardiol 21:37–46
21. Paz R, Mohiaddin RH, Longmore DB (1993) Magnetic resonance assessment of the pulmonary arterial trunk anatomy, flow, pulsatility and distensibility. Eur Heart J 14:1524–1530
22. Snider AR, Enderlein MA, Teitel DR et al (1984) Two-dimensional echocardiographic determination of aortic and pulmonary artery sizes from infancy to adulthood in normal subjects. Am J Cardiol 53:218–224
23. Wu MT, Huang YL, Hsieh KS et al (2007) Influence of pulmonary regurgitation inequality on differential perfusion of the lungs in tetralogy of Fallot after repair. A phase-contrast magnetic resonance imaging and perfusion scintigraphy study. J Am Coll Cardiol 49:1880–1888
24. Kang IS, Redington AN, Benson LN et al (2003) Differential regurgitation in branch pulmonary arteries after repair of tetralogy of Fallot, a phase-contrast cine magnetic resonance study. Circ 107:2938–2943
25. Sridharan S, Derrick G, Deanfield J et al (2006) Assessment of differential branch pulmonary blood flow: a comparative study of phase contrast magnetic resonance imaging and radionuclide lung perfusion imaging. Heart 92:963–968
26. Kisslo J, Adams D, Mark D (1988) Basic Doppler echocardiography. Churchill Livingstone, New York
27. Labovitz A (1988) Doppler echocardiography. Lea & Febinger, Philadelphia
28. Gardin J, Burn CS, Childs WJ et al (1984) Evaluation of blood flow velocity in the ascending aorta and main pulmonary artery of normal subjects by Doppler echocardiography. Am Heart J 107:310–319
29. Frigiola A, Redington AN, Cullen S et al (2004) Pulmonary regurgitation is an important determinant of right ventricular contractile dysfunction in patients with surgically repaired tetralogy of Fallot. Circ 110:153–157
30. Reiter G, Reiter U, Kovacs G et al (2008) Magnetic Resonance derived 3-dimensional blood flow patterns in the main pulmonary artery as a marker of pulmonary hypertension and a measure of elevated mean pulmonary arterial pressure. Circ Cardiovasc Imaging 1:23–30
31. Frydrychowicz A, Berger A, Russe MF et al (2008) Time-resolved magnetic resonance angiography and flow-sensitive 4-dimensional magnetic resonance imaging at 3 Tesla for blood flow and wall shear stress analysis. J Thorac Cardiovasc Surg 136:400–407
32. Frydrychowicz A, Arnold R, Hirtler D et al (2008) Multidirectional flow analysis by cardiovascular magnetic resonance in aneurysm development following repair of aortic coarctation. J Cardiovasc Magn Reson 10:30
33. Therrien J, Siu SC, McLaughlin PR et al (2000) Pulmonary valve replacement in adults late after repair of tetralogy of Fallot: are we operating too late? J Am Coll Cardiol 36:1670–1675
34. Park CS, Lee JR, Lim HG et al (2010) The long term result of total repair of tetralogy of Fallot. Eur J Cardio Thorac Surg 38:311–317
35. Jung B, Honal M, Ullmann P et al (2008) Highly k-t-space-accelerated phase-contrast MRI. Magn Reson Med 60:1169–1177